J. Physiol. (1981), **312**, *pp.* 159–176
With 12 text-figures
Printed in Great Britain

SLOW CALCIUM AND POTASSIUM CURRENTS ACROSS FROG MUSCLE MEMBRANE: MEASUREMENTS WITH A VASELINE-GAP TECHNIQUE

BY W. ALMERS AND P. T. PALADE†

From the Department of Physiology and Biophysics, University of Washington, SJ-40, Seattle, WA 98195, U.S.A.

(*Received 16 May 1980*)

SUMMARY

1. A vaseline-gap voltage-clamp technique was used to record slow Ca^{2+} and K^+ currents from frog skeletal muscle fibres loaded with the Ca^{2+} chelator EGTA.

2. K^+ currents were increased when Mg^{2+} replaced external Ca^{2+}, and they were abolished when internal K^+ was replaced by tetraethylammonium (TEA^+). Ca^{2+} currents could be studied in isolation in fibres loaded with $(TEA)_2EGTA$.

3. Under maintained depolarization, Ca^{2+} currents slowly increase (half-time of 35 msec or more at 25 mV) and then decline to a steady value. Decline under repolarization is rapid (half-time of 6–7 msec) and complete. During an action potential, the Ca^{2+} influx through this system is probably less than the influx observed with tracers.

4. Ba^{2+}, Sr^{2+}, Ca^{2+}, Mn^{2+} and Mg^{2+} can carry current across the membrane; Ni^{2+} and Co^{2+} cannot. Ca^{2+} currents are weakly blocked by external Mg^{2+}.

INTRODUCTION

Many cell membranes respond to depolarization with an increase in permeability to Ca^{2+} ions, which is sometimes sufficient to result in electrical excitation (Hagiwara, 1975; Reuter, 1973). Presumably, the increase in Ca^{2+} permeability happens by voltage-dependent opening (gating) of 'Ca^{2+} channels', as yet hypothetical macromolecules in the membrane capable of transporting Ca^{2+}. Although Ca^{2+} channels seem to occur in most membranes where Ca^{2+} currents have been looked for, detailed information about them has emerged only slowly. A significant advance was the combination of voltage clamp and internal dialysis, applied successfully to snail neurones by Kostyuk & Krishtal (1977) and Akaike, Fishman, Lee, Moore & Brown (1978). With the new method, it was possible to record what are believed to be 'gating currents' in Ca^{2+} channels (Krishtal & Pidoplichko, 1976; see also Adams & Gage, 1979) and to measure the conductance of a single open Ca^{2+} channel (Kostyuk, Kirshtal & Pidoplichko, 1978; Akaike *et al.* 1978).

Among vertebrate tissues skeletal muscle offers favourable conditions. Skeletal muscle can generate Ca^{2+}-mediated action potentials (Beaty & Stefani, 1976) and sizeable Ca^{2+} currents under voltage clamp (Stanfield, 1977; Sanchez & Stefani, 1978);

† Present address: Department of Molecular Biology, Vanderbilt University, Nashville, TN 37235, U.S.A.

0022-3751/81/3580-0974 $07.50

furthermore, a voltage-clamp technique allowing control of intracellular ion content is available (Hille & Campbell, 1976). In this paper and the next (Almers, Fink & Palade, 1981) we use the Hille–Campbell method to study Ca^{2+} currents under conditions where they can be observed in isolation. Here we report observations concerning time and voltage dependence of Ca^{2+} conductance, and explore the permeability of several divalent cations. Some of the present results were included in a preliminary report (Palade & Almers, 1978).

METHODS

Preparation and voltage clamp

The recording chamber and voltage clamp were of the Hille & Campbell (1976) design. Fig. 1 (top) shows, approximately to scale, a piece cut from a single muscle fibre (stippled). Three 150–200 μm thick threads of vaseline are laid across the fibre in order to define four separate electrolyte pools (A, B, C. E). The arrangement serves to isolate electrically the 350–450 μm long section in the A pool. This section is ultimately bathed in one of our external solutions (Table 1) while the cut ends on either side are soaking in 'intracellular' solution, in our case isotonic solutions of the Ca^{2+} chelator, ethyleneglycol-bis-(β-aminoethylether) *N,N'*-tetraacetate (EGTA). The potential across the cell membrane in the A pool can be recorded through the cut end in the C pool. B and C pools are kept isopotential by electronic feed-back in order to prevent currents which may flow between A and C pools and dissipate the membrane potential. By injecting current through the cut end in the E pool, the section in the A pool may be voltage-clamped.

Pieces of single fibres were dissected in isotonic K_2EGTA or (K_2SO_4 + 10 mM-$CaSO_4$) solutions from the dorsal head of semitendinosus muscles of the english frog, *Rana temporaria*. After the fibre segment was mounted in the chamber, fibre ends in C and E pools were cut to a length not exceeding 0·5 mm. The voltage-measuring amplifier was balanced with all liquid-junction electrodes in place and all pools of the chamber coalesced by flooding with internal solution (isotonic solutions of either K_2EGTA or (tetraethylammonium)$_2$EGTA). After the pools were separated by lowering the solution level, the potentiometric feed-back loop was activated and the membrane potential was taken, without further rebalancing, as equal to the output of the voltage-measuring amplifier. External solution (usually containing 10 mM-Ca^{2+}) was then applied, and the fibre section in the A pool voltage-clamped with the holding potential set to −70 mV. After a suitable equilibration period (at least 30 min after cutting fibre ends when the internal solution was (TEA)$_2$EGTA) the experiment could start. Temperature was 20–24 °C throughout.

Recording

Membrane current was taken as equal to the current flowing into the E pool and was measured either as the voltage drop across at 10 kΩ resistor or that across a 250 kΩ resistor placed in the feed-back loop of a current-measuring circuit in series with the E pool. Current was corrected in a preliminary way for leakage and capacitive currents by means of an analogue 'transient generator' or 'leak subtractor' (e.g. Armstrong & Bezanilla, 1975, or Hille & Campbell, 1976). This device could be set to simulate current during 10 mV de- or hyperpolarizing pulses, and then to subtract appropriately scaled versions of this signal from currents during larger pulses. Membrane current corrected in this way, as well as the voltage, were passed through a four-pole Bessel low-pass filter (Frequency Devices, Haverhill, Mass.) with corner frequency set to 100 Hz. Current and voltage were then amplified and sampled at 100 Hz (unless otherwise indicated) each by twelve-bit A/D converter (Analogics, Wakefield, Mass.). After conversion, membrane voltage and current were stored in digital form on magnetic tape in groups of 512 successive samples, each group called a 'trace'. This and other digital operations were done by an LM[2] minicomputer built and maintained by Dr Theodore Kehl and associates in this department. To record membrane currents during a voltage pulse of amplitude P ('test pulse'), the following procedure was used. The holding potential was temporarily set to −80 mV and four 'control pulses' were applied, each of amplitude $P/4$ and the same duration as the test pulse. The resulting eight traces (four each for voltage and current) were combined into two by signal-averaging. If the leak subtractor was set carefully, the resulting current trace was flat. The holding potential was then returned to −70 mV, and current and

voltage during the 'test pulse' were sampled. Voltage and current during both test and control pulses were stored separately for later analysis. Current during the test pulse, I_T, could be corrected for any leakage and capacitive contributions that escaped cancellation by the leak subtractor by forming

$$I = I_T - V_T I_C / V_C, \quad (1)$$

where I_C is the (signal averaged) current during the control pulse and V_T and V_C the measured amplitudes of test and control pulse, respectively, their ratio being approximately four. With this method, most of the noise in I is contributed by the I_C measurement, since the signal-to-noise ratio of I_C is typically half of that of I_T. Therefore voltage and I_C traces of three to four successive sequences of control and test pulses were often signal-averaged and used in eqn. (1) to achieve a final correction for leak and capacitive currents.

Solutions

Internal solutions contained either 80 mM-K_2EGTA or 80 mM-(tetraethylammonium)$_2$-EGTA ((TEA)$_2$EGTA), made from EGTA (acid) by titration to pH 7 or 7·2 with KOH or (TEA)OH. Internal solutions filled the B pool and bathed the cut ends of the fibre in C and E pools (Hille & Campbell, 1976).

The composition of *external solutions* is shown in Table 1. They were designed to be free of Cl^-, K^+ and Na^+. Most Ca^{2+}-containing solutions were made by mixing two stock solutions (solutions 2 and 3) in the correct proportions; one contained 100 mM-calcium methanesulphonate ($MeSO_3$) and the other approximately 120 mM-TEA^+ $MeSO_3$. The solutions were made by neutralizing methane-sulphonic acid (Aldrich Chemical Co., Milwaukee, Wis., or MCB, Norwood, Ohio) with TEA^+ hydroxide (B.D.H. Chemicals Ltd, Poole, England or Aldrich Chemical Co., Milwaukee, Wis.) or $Ca(OH)^2$. Both were isotonic with Ringer fluid to within 10 % as measured with a vapour pressure osmometer (Wescor, Logan, Utah). Ca^{2+} activities were measured with a Ca^{2+}-sensitive electrode (Orion Research Co., Cambridge, Mass.). In some experiments, the external solution contained 10 mM-$CaCl_2$, $BaCl_2$, $SrCl_2$ or $MnCl_2$ in place of $Ca(MeSO_3)_2$ (solutions 5 and 6). The Ba^{2+}, Sr^{2+} and Mn^{2+} activities in our solutions are not accurately known. We also measured the Ca^{2+} activities of Ringer fluid (0·65 mM, soln. A) and sulphate Ringer (2 mM, soln. D); the indices A and D refer to Table 1 of Hodgkin & Horowicz (1959) where the composition of these two solutions is given. All external solutions were buffered to pH 7·0–7·2 by adding 3 mM-TEA morpholinopropane-sulphonate (Calbiochem, La Jolla, California).

Immobilization of muscle fibres

The contractile response to cell membrane depolarization was abolished by cutting fibre ends in solutions containing high concentrations (80 mM) of EGTA. Fluoride would have been as effective as EGTA in blocking contraction, but in our experience greatly reduced or abolished Ca^{2+} currents (see also Kostyuk & Krishtal, 1977). In addition to being cut in EGTA, most semitendinosus muscles were soaked for 15–36 hr in 80 mM-K_2EGTA + 5 mM-Na_2ATP at 8 °C before and during the dissection of single fibres from them. This treatment in itself abolished (or severely reduced) contraction due to cell membrane depolarization, probably because fibres so treated have lost most of their exchangeable intracellular Ca^{2+} (see Curtis, 1966). Occasionally, fresh muscles were used; if so, they were dissected in a buffered solution (pH 7) containing 10 mM-$CaSO_4$ and 95 mM-K_2SO_4. Thirty minutes or more were allowed for diffusion of K_2EGTA or (TEA)$_2$EGTA through the cut fibre ends. Use of fresh muscles is indicated in the Figure legend.

Properties of fibres soaked in 80 mM-K_2EGTA

Such fibres have clearly visible striations under the light microscope and a normal sarcomere length. They are relaxed, depolarized ($V_m \sim 5$ mV) and compliant. Micro-electrode measurements were made on one muscle soaked for 17–18 hr in K_2EGTA; cable analysis on three fibres in this solution gave the following results, ±S.E. of mean: length constant $\lambda = 1{\cdot}47 \pm 0{\cdot}04$ mm, internal resistance $r_i = 1{\cdot}17 \pm 0{\cdot}11$ MΩ/cm, membrane resistance $r_m = 25{\cdot}1 \pm 2{\cdot}1$ kΩ/cm. Assuming an average diameter of 80 μm, the membrane conductance becomes $G_m = 1{\cdot}61 \pm 0{\cdot}12$ mS/cm^2. Assuming instead a normal internal resistivity (169 Ω m, Hodgkin & Nakajima, 1972*a*), one obtains $G_m = 0{\cdot}94 \pm 0{\cdot}05$ mS/cm^2 and an average fibre radius $a = 68 \pm 3$ μm. When the muscle was put into our standard 10 mM-Ca^{2+} saline, membrane conductance diminished about tenfold. Cable parameters for four fibres held at −100 mV were $\lambda = 4{\cdot}39 \pm 0{\cdot}75$ mm, $r_i = 3{\cdot}6 \pm 0{\cdot}7$ MΩ/cm and

TABLE 1. Composition of external solutions

No.	Solution reference	Ca^{2+} (mM)	TEA^{+} (mM)	Other (mM)	$CH_3SO_3^-$ (mM)	Cl^- (mM)	Ca^{2+} activity (mM)	Ca^{2+} activity referred to Ringer fluid
1	10 mM-Ca^{2+}	10	108	—	128	—	3·6	5·8
2	100 mM-Ca^{2+}	100	—	—	200	—	35·0	56
3	0 mM-Ca^{2+}	0	120	—	120	—	0·035*	0·056*
4	x mM-Ca^{2+}	Made by appropriately mixing solutions 2 and 3					†	†
5	10 mM-Mg^{2+}	0	105	Mg^{2+} (10 mM)	120	—	0·035*	0·056*
6	10 mM-Ca^{2+}–90 mM-Mg^{2+}	10	—	Mg^{2+} (90 mM)	200	—	—	—
7	10 mM-$CaCl_2$	10	105	—	—	105	20	—
8	10 mM-Ba^{2+}, Sr^{2+} or $MnCl_2$	—	105	Ba^{2+}, Sr^{2+} or Mn^{2+} (10 mM)	105	20	—	—

* Due to contamination of reagents. Ca^{2+} activity vanishes when EGTA is added.

† Ca^{2+} activities of these solutions grow linearly with $[Ca^{2+}]$ up to 10 mM.

$r_m = 0{\cdot}92 \pm 0{\cdot}47$ MΩ cm. Assuming $a = 40$ μm one has $G_m = 0{\cdot}11 \pm 0{\cdot}05$ mS/cm², assuming instead a normal internal resistivity (169 Ω cm), one obtains $G_m = 0{\cdot}090 \pm 0{\cdot}033$ mS/cm² and $a = 42{\cdot}7$ μm. These values for G_m in 10 mM-Ca^{2+} are similar to the three values given by Sanchez & Stefani (1978) for fibres in their sulphate solution (0·07, 0·08 and 0·12 mS/cm²).

When soaked fibres are mounted in the vaseline gap with 80 mM-K_2EGTA in extra- and intracellular pools, resting membrane conductance measured with ±10 mV pulses is about

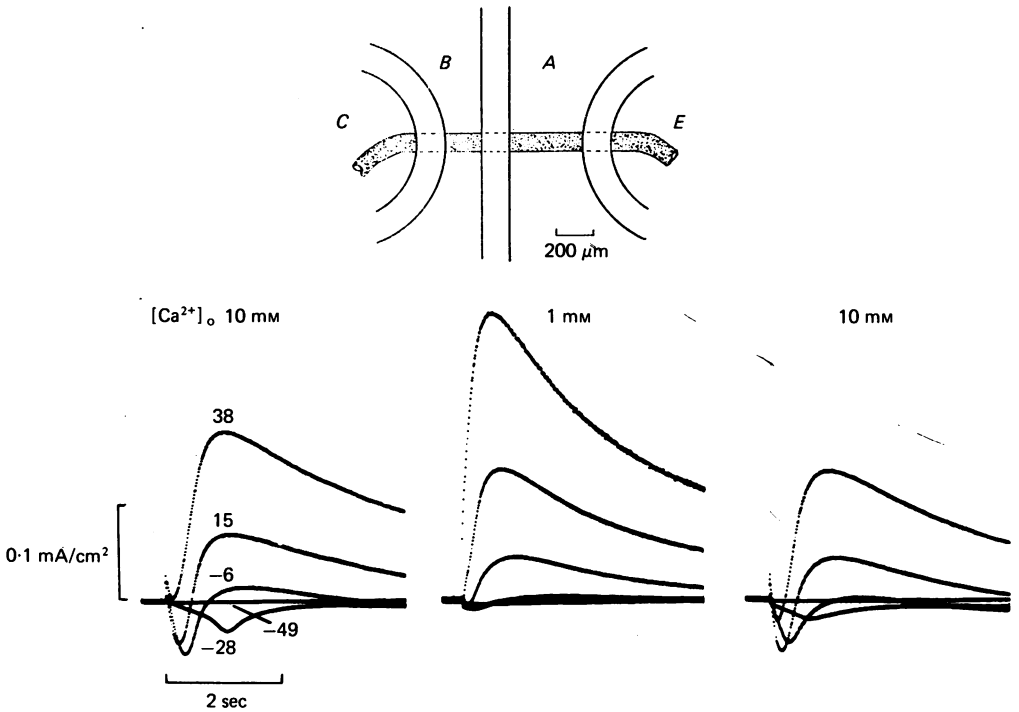

Fig. 1. Top: Schematic drawing of fibre (stippled) with vaseline seals dividing our experimental chamber into four pools, A, B, C and E. Drawing approximately to scale. Bottom: Membrane currents during step depolarizations to the potentials indicated; numbers are in mV. Internal: 80 mM-K_2EGTA; external: 10 and 1 mM-Ca^{2+} as indicated. Fibre 1512; diameter 100 μm.

1 mS/cm². With Ringer's fluid in the extracellular compartment and fibres held at −90 mV, one can elicit action potentials and, under voltage clamp, normal Na^+ and K^+ currents of the kind described by Adrian, Chandler & Hodgkin (1970*a*) and Hille & Campbell (1976; Na currents only). In our standard external 10 mM-Ca^{2+} solution no such action potentials or Na^+ currents are observed, and delayed K^+ currents are small or absent. Resting (or leakage) conductances at the holding potential of −70 mV are between 0·2 and 0·4 mS/cm², higher than we measured with micro-electrodes. Cutting fibre ends in 80 mM-$(TEA)_2$EGTA leads to no decrease in leakage conductance. In this case, none of the ions present intra- and extracellularly are expected to be permeant across the resting membrane, so it is likely that the 0·2–0·4 mS/cm² are almost entirely artifactual. Indeed, leakage of current underneath the vaseline seal between E and A pools (see Hille & Campbell, 1976) of the expected magnitude (3–4 MΩ for a typical vaseline seal) would appear as a leakage conductance of 0·26–0·4 mS/cm² in a typical preparation with gap width 0·4 mm and fibre diameter 100 μm. These values would correspond to leakage currents of 18–28 μA/cm² during depolarization from −70 mV to 0 mV, roughly quarter to half the size of a normal peak Ca^{2+} current at 0 mV. If the leakage conductance arises underneath the E–A seal, it is expected to be highly linear, since large electric fields do not exist there, and since the conductivities of intra- and extracellular solutions are not expected to differ greatly.

In summary, the prolonged soak in 80 mM-K_2EGTA has no significant effects on the membrane

properties of interest here. Membrane currents measured with the vaseline-gap method are contaminated by leakage currents larger than those recorded with micro-electrodes; but the leakage admittances may be expected to be ohmic, and can, therefore, be corrected for.

RESULTS

Slow Ca^{2+} and K^+ currents across skeletal muscle membrane

Fig. 1 (left) shows membrane currents recorded from a muscle fibre bathed in our standard 10 mM-Ca^{2+} external solution. Due to absence of external Na^+ and presence of TEA^+ in large concentration (about 110 mM), depolarizing steps to potentials ranging from −49 to +38 mV failed to elicit the rapid Na^+ and K^+ currents forming

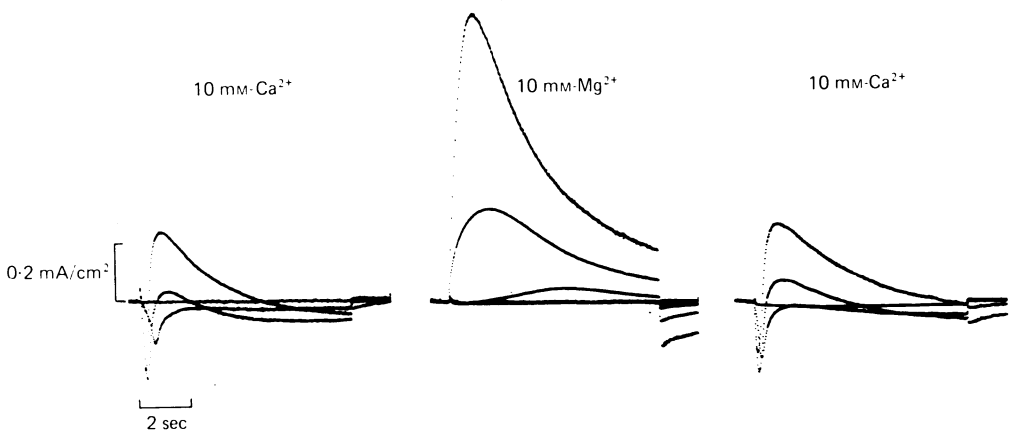

Fig. 2. Membrane currents during step depolarizations as in Fig. 1. Internal: 80 mM-K_2EGTA; external: 10 mM-Ca^{2+} or 10 mM-Mg^{2+} as indicated. Fibre 1504, diameter 130 μm, A pool width 290 μm.

the basis for normal membrane excitability. Instead one observes voltage-dependent inward and outward currents varying slowly with time. With internal K^+ and external Ca^{2+} as the only ions expected to be permeant, the inward current is probably carried by Ca^{2+} and the outward current by K^+. When external Ca^{2+} concentration is reduced tenfold (Fig. 1, middle) or replaced by Mg^{2+} (Fig. 2, middle), inward current is reversibly reduced or abolished, confirming that the inward current is carried by Ca^{2+}. Inward current is also insensitive to tetrodotoxin (not shown), but reduced or abolished by external application of substances generally thought to block Ca^{2+} channels, such as Co^{2+}, Ni^{2+}, D-600 or nifedipine (Almers *et al.* 1981, W. Almers and P. T. Palade, unpublished).

Magnitude and time course of inward current varied widely from fibre to fibre, with rapid kinetics usually found in fibres with large currents. In thirty-nine fibres, mean peak current amplitude during pulses to 0–5 mV ranged from −28 to −143 μA/cm^2 (mean ± S.D. was −74 ± 28 μA/cm^2, about fifty times smaller than peak Na^+ currents in Ringer solution), and time to peak ranged from 140 to 710 msec (mean ± S.D. was 340 ± 130 msec). This range encompasses the values observed by Sanchez & Stefani (1978) and Stanfield (1977) on intact fibres bathed in a solution with roughly half the Ca^{2+} activity of the present one (see Methods). In summary, we believe our inward

currents to be carried by Ca^{2+} and to flow through the channel investigated by Sanchez & Stefani (1978). Fig. 2 suggests that Mg^{2+} is much less permeant than Ca^{2+}; this point will be taken up again later.

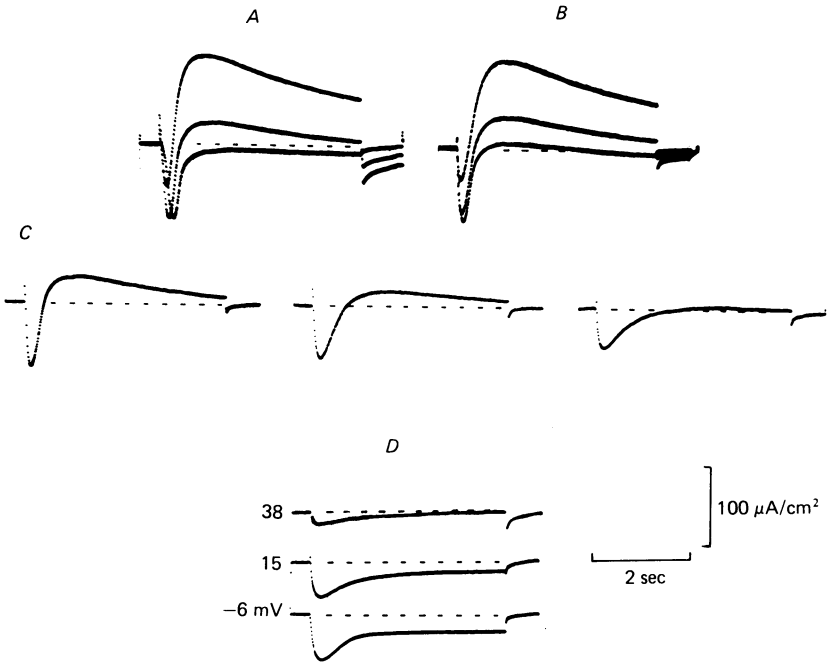

Fig. 3. Membrane currents during step depolarizations to 15 mV (*C*) or, from top to bottom, to 38, 15, and −6 mV (*A*, *B*, *D*). External: 10 mM-Ca^{2+}; internal: 80 mM-K_2EGTA (*A* and *B*) and later 80 mM $(TEA)_2$EGTA; see text for details. Currents in *C* were recorded 1, 5, and 11 min after changing from K^+ to TEA^+ in the pools bathing the cut ends. A pool width 350 μm; fibre ends were 0·9 mm and 1·3 mm from the edges of the A pool. Fibre 1527, diameter 140 μm.

The experiment in Figs. 3 and 4 investigates the ionic nature of the late outward current. Fig. 3*A* and *B* shows currents under the same conditions as in Figs. 1 and 2 (left), that is, with 80 mM-K_2EGTA solution bathing the cut ends of the fibre. The two sets of records were taken with a 20 min interval; no significant change occurred during that time, indicating that the rate of spontaneous 'rundown' is fairly slow. After the currents in *A* and *B* were recorded, all K^+ was exchanged for TEA^+. As TEA^+ replaced intracellular K^+ by diffusion through the cut ends, inward and outward currents at 15 mV diminished progressively (traces in Fig. 3*C*). After 25 min, the traces in Fig. 3*D* were recorded with potential steps as in Fig. 3*A*. Outward current is essentially abolished. Similar records are obtained when the cut ends are bathed in 80 mM-(tetramethylammonium$^+$)$_2$EGTA solution (not shown). These results confirm that K^+, but not TEA^+ or tetramethylammonium$^+$, can carry outward currents of the type seen in Figs. 1–3. With Cs^+ replacing K^+ internally, outward currents are up to threefold smaller but of similar time course (not shown). Fig. 4 analyses the experiment of Fig. 3, plotting maximal outward current at 38 mV (filled

circles) and peak inward current at 15 mV (open circles) against time. At the arrow, TEA^+ was substituted for K^+ in the solution bathing the cut ends of the fibre. Outward current disappeared almost totally, and peak inward current declined by 30–50 %.

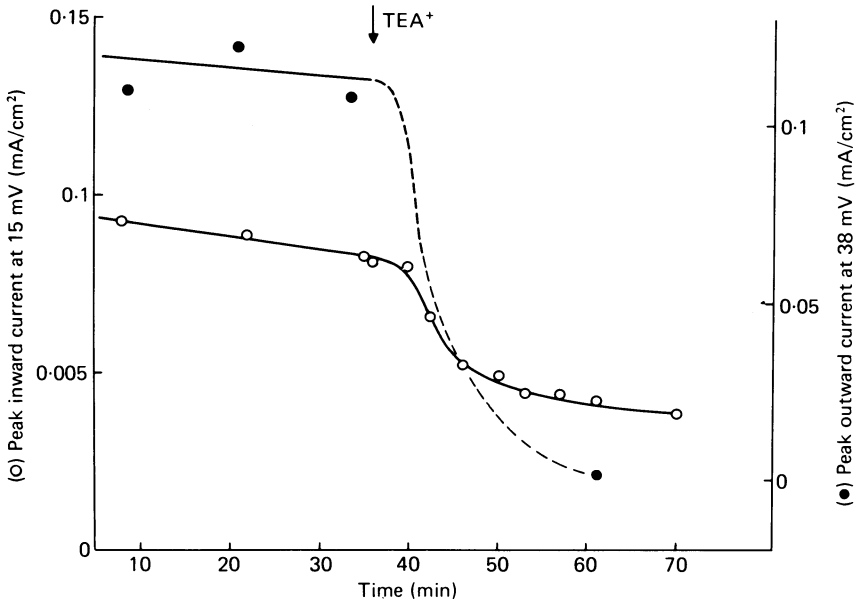

Fig. 4. Peak outward current at 38 mV (●) and peak inward current at 15 mV (○) in the experiment of Fig. 3. The solutions bathing the fibre ends were changed at the time indicated to replace internal K^+ with TEA^+.

The ion substitution experiments described so far are consistent with the inward current being carried by Ca^{2+} and the outward current by K^+. They also show, however, that effects on the two currents are not selective. Internal TEA^+ at the high concentrations employed here (160 mM) diminishes I_{Ca^+}, probably acting as a weak Ca^{2+}-channel blocker. Partial withdrawal of external Ca^{2+} in Fig. 1 causes an increase in outward current, suggesting that the ionic channel involved here is blocked by Ca^{2+}. M^{2+} evidently is less effective, or ineffective, as a blocking ion (Fig. 2). Similar results with Mg^{2+} were also obtained in fresh fibres (R. Fink & W. Almers, unpublished).

Effects of external Ca^{2+} and Mg^{2+}

In all remaining experiments, late outward currents were prevented by cutting fibre ends in 80 mM-$(TEA)_2$EGTA. After 30 min equilibration, depolarizations to potentials up to 30 mV (indicated on the left in Fig. 5) produce an inward current declining incompletely, but no outward current. Stable records of this kind can be obtained for up to an hour, and we believe them to be essentially pure Ca^{2+} currents. The fibre in Fig. 5 was of relatively small diameter and produced small currents; this is expected to minimize potential non-uniformities if a large portion of I_{Ca} flows through the transverse tubules. In such fibres I_{Ca} ends abruptly upon repolarization, at least on this time scale, and peak amplitude increases gradually as the amplitude of depolarization is increased (see current–voltage curves in Fig. 6). In many other

fibres, I_{Ca} instead showed a clear threshold potential with depolarizations of the critical amplitude producing, after a delay, explosive and seemingly regenerative inward currents. Repolarization in such fibres often produced an inward 'tail' of I_{Ca}

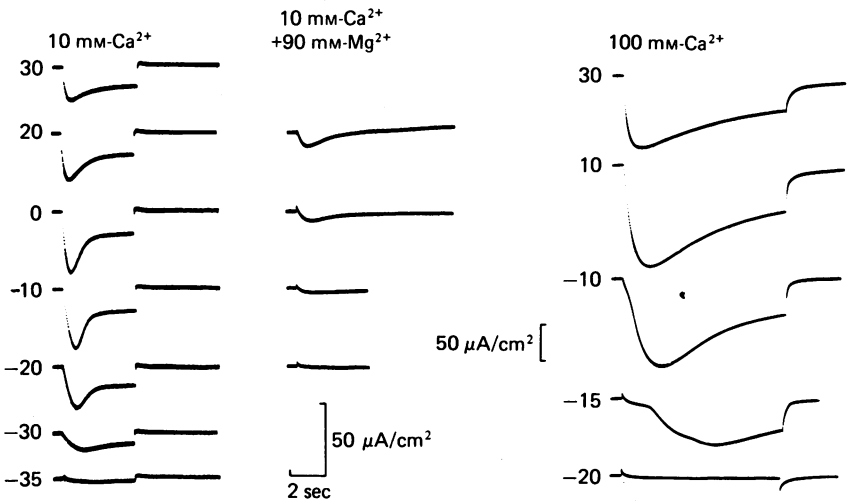

Fig. 5. Membrane currents during depolarizations to the potentials indicated next to traces; the figures on the left apply to left and middle column of traces. Internal: $(TEA)_2EGTA$; external: 10 mM-Ca^{2+}, 10 mM-Ca^{2+} + 90 mM-Mg^{2+} and 100 mM-Ca^{2+} as indicated. Current traces recorded at the end of the experiment upon return to 10 mM-Ca^{2+} can be seen in Fig. 8 of Almers *et al.* 1981. Fresh fibre 14–1; diameter 63 μm.

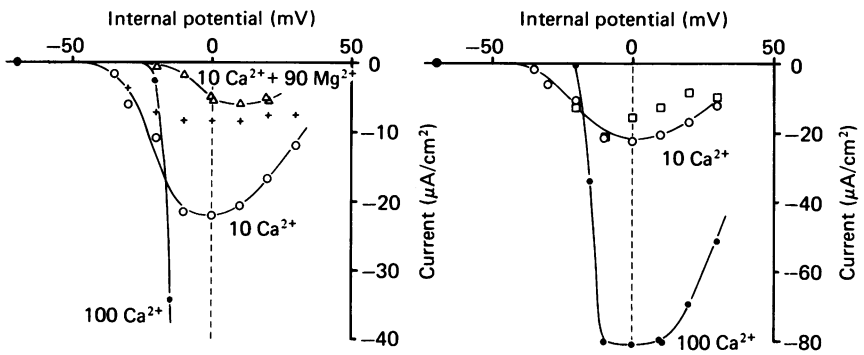

Fig. 6. Current–voltage curves from the experiment of Fig. 5. Left: peak currents in 10 mM-Ca^{2+} (○), 10 mM-Ca^{2+} + 90 mM-Mg^{2+} (△) and 100 mM-Ca^{2+} (●); crosses give final currents in 10 mM-Ga^{2+}. Right: peak currents in 10 mM-Ca^{2+} before (○) and after (□) exposure at 100 mM-Ca^{2+} (●).

declining with time constants (20–100 msec) which were clearly correlated with the current immediately before repolarization. We interpret such effects as being due to potential non-uniformities, probably in the transverse tubular system.

Fig. 6 (left) plots peak (circles) and final current (crosses) against potential. Peak currents seem to extrapolate to a zero current potential of +50 mV; however, when this was tested with pulses to 50 mV (other experiments, not shown), I_{Ca} at 50 mV

was still inward. With 80 mM intracellular EGTA, outward I_{Ca} is not expected, and outward currents kinetically resembling the traces in Fig. 5 (left) were never observed. It seems reasonable, therefore, to assume that under conditions as in Figs. 5 and 6 the reversal potential of the Ca^{2+} channel is so far positive as to be experimentally inaccessible, and that the currents in Fig. 5 therefore represent essentially unidirectional Ca^{2+} influx.

When all external TEA^+ is replaced by Mg^{2+} on an isosmolar basis (middle column of traces in Fig. 5), inward currents become smaller, and larger depolarizations are needed to turn them on. In isotonic Ca^{2+}-methanesulphonate (right column in Fig. 5) currents are large again, but one needs to depolarize beyond -20 mV to elicit them. The irregular time course of current at -15 mV is probably due to regenerative responses in the transverse tubular system. Current–voltage curves of this experiment are plotted in Fig. 6 (left), showing peak currents in 10 mM-Ca^{2+} (circles), in 10 mM-Ca^{2+} + 90 mM-Mg^{2+} (triangles) and in 100 mM-Ca^{2+} (dots). Fig. 6 (right) shows peak voltage currents in 10 mM-Ca^{2+} (circles), 100 mM-Ca^{2+} (dots) and after return to 10 mM-Ca^{2+} (squares).

The experiments of Figs. 5 and 6 illustrate several effects of Ca^{2+} and Mg^{2+}. (1) Mg^{2+} at high concentration blocks Ca^{2+} channels, perhaps by competing with Ca^{2+} for a site in the channel. (2) Increasing external Ca^{2+} concentration increases $I_{Ca^{2+}}$, but the increase is much less than proportional. Evidently, ion transport through the Ca^{2+} channel shows saturation. (3) Increasing external Ca^{2+} or Mg^{2+} concentrations shifts the potential dependence of Ca^{2+} conductance to more positive potentials, a change from 10 mM to 100 mM producing a shift of about 20 mV. The effect is similar to that observed with other ionic channels subject to 'gating' by the electric field in the membrane, and probably results from changes in the external membrane surface potential (Frankenhaeuser & Hodgkin, 1957; Hille, Woodhull & Shapiro, 1975). Similar effects are expected with all other divalent cations. (4) There are changes in time course; in particular, the decline of current is slowed in Mg^{2+} and high Ca^{2+} (compare traces at -10 and 0 mV). These effects are further discussed in the following paper (Almers *et al.* 1981).

Selectivity of Ca^{2+} channel

Several other divalent cations can carry inward currents. Fig. 7 shows currents first with 10 mM-Ca^{2+}, then with 10 mM-Ba^{2+}, and again with 10 mM-Ca^{2+} in the external solution. In Ba^{2+} the kinetics are accelerated and inward current increased (note different abscissa and ordinate scales). There is also an indication that the voltage dependence of Ca^{2+} currents is shifted to 10–20 mV more negative potentials (four experiments); part of the effect could be explained if the activity of Ba^{2+} is less than that of Ca^{2+} in the solutions employed here. The conclusion from Fig. 7 is that Ba^{2+} is more permeant than Ca^{2+}.

Small inward currents remained when Ca^{2+} was replaced by Mg^{2+} (Fig. 8). They were smaller than outward leakage currents at the same potentials (subtraced in Fig. 8) so that 'action potentials' would not be expected under this condition. In four fibres, peak inward currents in Mg^{2+} at -10 mV were $3{\cdot}3 \pm 0{\cdot}6$ $\mu A/cm^2$ ($\pm$S.E.M. of mean), and their size relative to those recorded in 10 mM-Ca^{2+} was $0{\cdot}10 \pm 0{\cdot}03$. They are unlikely to be due to Ca^{2+} contamination of our 10 mM-Mg^{2+} solution, whose Ca^{2+}

activity was determined to be less than 43 μM, eighty times less than the Ca^{2+} activity of our 10 mM-Ca^{2+} solution. Repeated washing with this solution produced no further decrease of the currents in Fig. 8 (middle), and currents of a similar size were observed

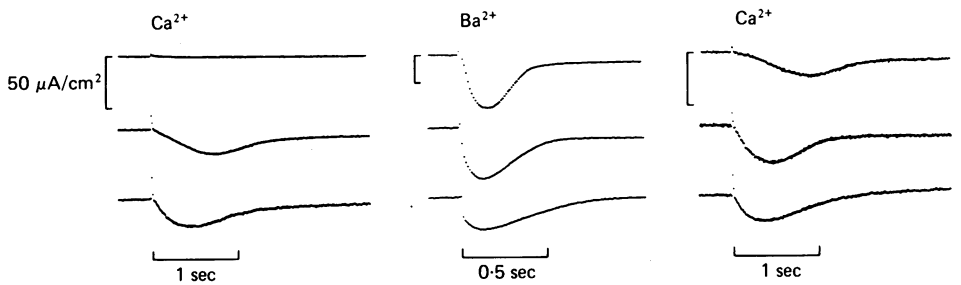

Fig. 7. Membrane currents during depolarizations to −27, −6, and 15 mV, from top to bottom. Internal: 80 mM-$(TEA)_2EGTA$; external: 10 mM-$CaCl_2$ or 10 mM-$BaCl_2$ as indicated. Note different abscissa and ordinate scales in the middle set of records. Fibre 1523, diameter 140 μm.

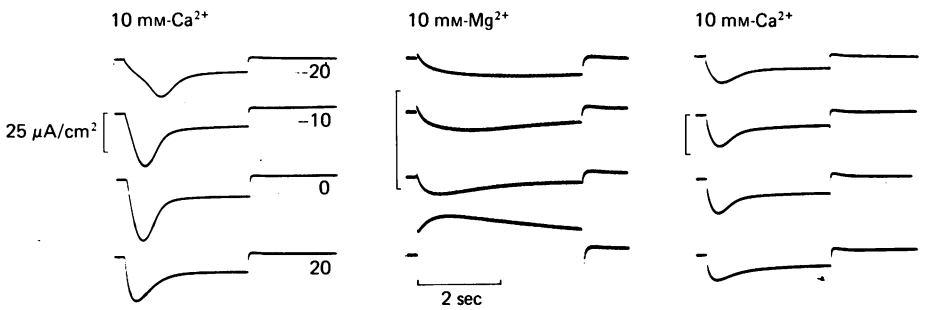

Fig. 8. Membrane currents during depolarizations as indicated. Internal: $(TEA)_2EGTA$; external: 10 mM-Ca^{2+} and 10 mM-Mg^{2+} as indicated. Note different ordinate scale for middle set of traces. Fresh muscle. Fibre 25–2, diameter 130 μm.

after the Ca^{2+} activity of our 10 mM-Mg^{2+} solution was reduced to below 50 mM by adding 0·8 mM-$(TEA)_2EGTA$. Experiments in Ca^{2+}-free solutions are complicated by the presence of a depolarization-activated permeability mechanism which allows transport of all alkali metal ions and is blocked by external Ca^{2+} but not Mg^{2+} (Palade & Almers, 1978; P. T. Palade & W. Almers, unpublished). The outward current seen in Fig. 8 (middle) at the most positive potential could be due to outward movements of residual internal K^+ via this permeability mechanism.

Figs. 9 and 10 show experiments with other divalent cations. In Fig. 9 external cations were, in succession, Ca^{2+}, Mn^{2+}, Ca^{2+}, Ni^{2+}, Ca^{2+}; in Fig. 10 they were Ca^{2+}, Sr^{2+}, Ca^{2+}, Co^{2+}, Ca^{2+}. Evidently, Sr^{2+} and Mn^{2+} carry inward currents, Co^{2+} and Ni^{2+} do not. (In Figs. 9 and 10 we attribute the small and abruptly developing currents in Ni^{2+} and Co^{2+} to leakage rectification). Judging by the relative size of currents at, e.g. 0 mV, the permeability sequence would be $Ba^{2+} > Sr^{2+} > Ca^{2+} > Mn^{2+} > Mg^{2+}$, with Ni^{2+} and Co^{2+} not being noticeably permeant. Ba^{2+} and Mn^{2+} were confirmed to be permeant also in fresh fibres (Almers *et al.* 1981; R. Fink & W. Almers,

unpublished). Reversal potential measurements might, if they were possible, produce different results. For instance, failure of Ni^{2+} and Co^{2+} to carry inward current is probably due, at least in part, to their well known ability to block Ca^{2+} channels

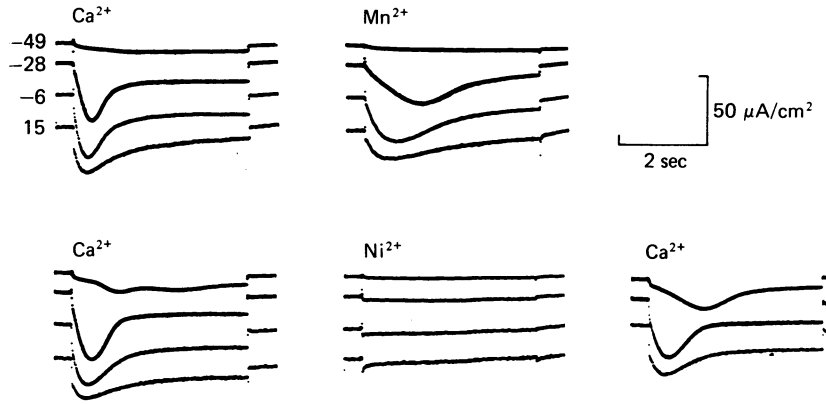

Fig. 9. Membrane currents during depolarizations to the potentials indicated (upper left). Internal: $(TEA)_2EGTA$; external: 10 mM-$CaCl_2$, 10 mM-$MnCl_2$ or 10 mM-$NiCl_2$ as indicated. Fibre 1521, diameter 160 μm.

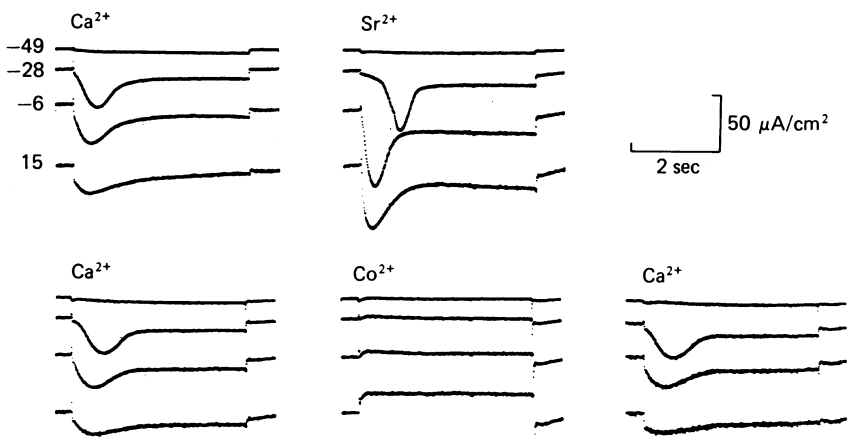

Fig. 10. As in Fig. 9 but with external 10 mM-$CaCl_2$, 10 mM-$SrCl_2$ and 10 mM-$CoCl_2$ as indicated. Fibre 1525, diameter 130 μm.

(unpublished, Almers *et al.* 1981). Mn^{2+} also blocks I_{Ca} (not shown); evidently Mn^{2+} can both block and carry current.

Voltage and time dependence of Ca^{2+} conductance

Fig. 11 shows Ca^{2+} currents during and after depolarization at a faster sweep speed. Depolarization is seen to produce a small transient outward current followed by inward $I_{Ca^{2+}}$. Repolarization elicits an inward 'tail' of $I_{Ca^{2+}}$ which declines rapidly as Ca^{2+} channels close. This inward current is well fitted by a declining exponential (Fig. 11*B*) with time constant of about 8–10 msec, fairly independently of the potential during the depolarizing pulse (Fig. 12, top) over a range of potentials where

the final current during depolarization (circles, Fig. 12, bottom) varied steeply. This suggests that potential non-uniformities due to I_{Ca} did not greatly affect this measurement, and that a value of about 10 msec may be taken to represent the time constant of channel closing at −70 mV. Other experiments gave higher values,

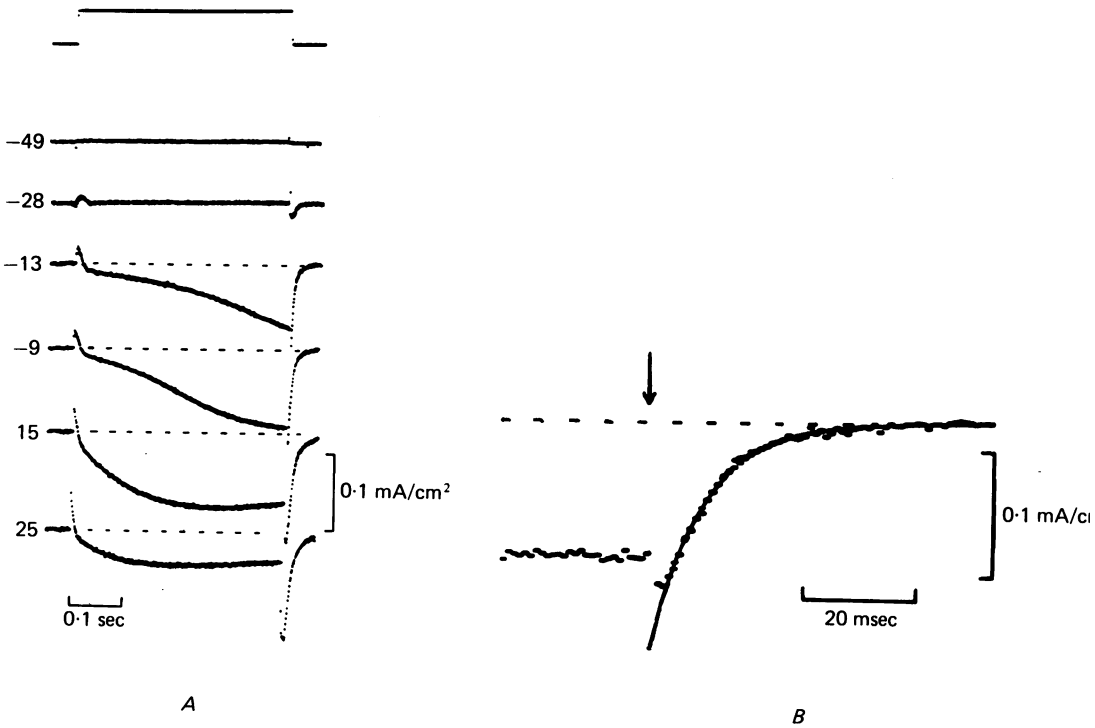

Fig. 11. (*A*), membrane potential (top) and currents (bottom) at the potentials indicated in mV. (*B*), membrane current upon repolarization from −9 to −70 mV (arrow); same record as in (*A*) but on an expanded abscissa. Continuous line is an exponential fitted to the decline of $I_{Ca^{2+}}$; its time constant is 8·7 msec. Sampling frequency and filter cut-off 1 kHz. External: 10 mM-Ca^{2+}; internal: 80 mM-$(TEA)_2$EGTA. A pool width 240 μm. Fibre 1170, diameter 120 μm.

possibly due to failure of the T-system to repolarize rapidly at the end of the pulse. Insofar as during the relatively short pulses employed here one may neglect the processes leading to the decline of $I_{Ca^{2+}}$ under maintained depolarization, one may take the amplitude of inward 'tails' as an index of the number of Ca^{2+} channels open at the end of the pulse (filled circles in Fig. 12). This measurement is expected to be more vulnerable to lack of potential control than was the measurement of decay time constant.

The initial outward transient is probably charge movement (Chandler, Rakowski & Schneider, 1976; Adrian & Almers, 1976). In order to isolate it, we fitted either straight lines or declining exponentials (depolarizations beyond 10 mV) to a 20–50 msec segment of the trace following the outward transient. The curve or line was extrapolated to the beginning of the pulse, subtracted, and the remaining

transient integrated with respect to time. The integral is plotted against potential in Fig. 12 (bottom squares). There is much scatter, since the experiment was not designed to study charge movements. Nevertheless, there is a suggestion of a voltage dependence similar to that of charge movements in intact fibres, with saturation at

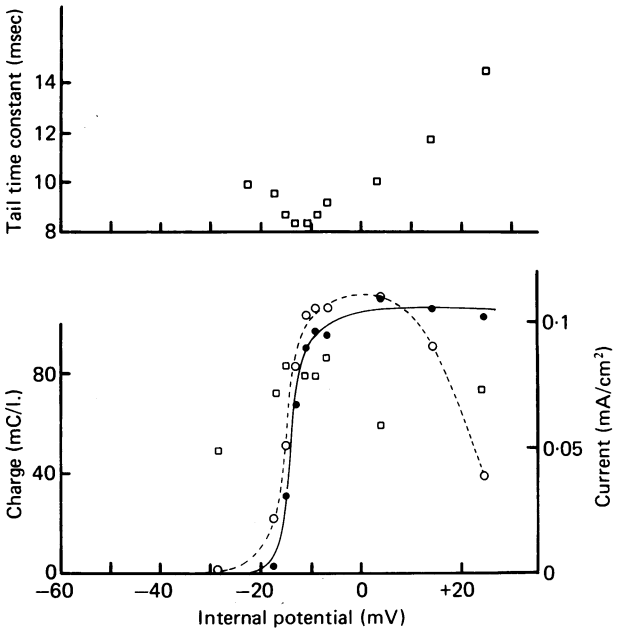

Fig. 12. Analysis of Fig. 11. Abscissa: potential during depolarizing pulse. Top: time constant describing decline of $I_{Ca^{2+}}$ upon repolarization. Bottom: (○) final inward current during pulses, (□) charge carried by the small outward current transient at the beginning of depolarizing pulses, (●) amplitude of inward tail current corrected for expected inward 'charge movement' by subtracting 35 and 40·2 μA/cm^2 from the measured amplitudes after pulses to −17 and −15 mV, and 35·5 μA/cm^2 from all other transients (for details see text). These values are proportional to the observed 'on' charge movements at the appropriate potentials (−17 and −15 mV) or to the average 'on' charge movement observed between −13 and 25 mV.

positive potentials and an asymptotic value of about 80 μC/cm^3 of fibre volume. With a membrane capacity of $2{\cdot}7 \times 10^3$ μF/cm^3 (Hodgkin & Nakajima, 1972*b*), this translates into a maximal charge movement of about 30 nC/μF, similar to values obtained in intact fibres.

To correct approximately for the contribution of charge movements to inward current after repolarization, we assumed the peak inward current at −20 mV to be entirely due to charge movements, and took the contribution at other potentials as being proportional to the charge voltage distribution (squares in Fig. 12, bottom). After subtracting these values from the tail amplitudes, we obtained the filled circles which may be taken as an estimate for the number of open Ca^{2+} channels at the end of pulses.

At positive potentials, net membrane currents are small, especially if a portion of the outward leakage currents (subtracted in Fig. 11) flows across the tubule

membrane and may thus be added to $I_{Ca^{2+}}$. This suggests that potential control in the transverse tubules may be sufficiently good to interpret the initial time course of $I_{Ca^{2+}}$ as representing the time course of channel opening. At 15 mV and 25 mV the section of traces where $I_{Ca^{2+}}$ is increasing (30–150 msec after depolarization) is reasonably well fitted by single exponentials with time constants of 78·9 and 55·4 msec, respectively. Another fibre gave a time constant of 110 msec at +30 mV. By approximating this time course by a single exponential, we do not wish to imply that Ca^{2+} channels obey first-order kinetics at these or other potentials.

In conclusion, Ca^{2+} channels are opened completely by depolarizations to positive potentials; they open with half-times of the order of 35–70 msec at 25–30 mV and close upon repolarization to −70 mV with half-times of the order of 7 msec.

DISCUSSION

We report here that the vaseline-gap voltage-clamp method (Hille & Campbell, 1976) can be used to record Ca^{2+} currents which are similar in time course and magnitude to those recorded from intact skeletal muscle fibres by Stanfield (1977) and Sanchez & Stefani (1978). In order to prevent contractions, EGTA at high concentration must be allowed to enter the fibre by perfusion through the cut ends. Soaking of muscles in K_2EGTA for 15–30 hr before use was also helpful, though not essential. Preliminary investigations show that fibres treated in this way contain many, perhaps all, the ionic channels found in intact fibres. We see two advantages in the vaseline-gap method. (1) It allows rapid exchange of external solutions. (2) It allows removal of internal K^+ and, consequently, the removal of contaminating outward currents carried by this ion. The method would also allow internal application of substances possibly influencing Ca^{2+} channels.

We have shown that Ca^{2+} channels in skeletal muscle are permeable, in order of permeability, to Ba^{2+}, Sr^{2+}, Ca^{2+}, Mn^{2+}, and possibly Mg^{2+}. Co^{2+} and Ni^{2+} are not measurably permeant. With regards to Ba^{2+}, Sr^{2+} and Ca^{2+}, our channel evidently behaves like others, such as in barnacle muscle (Hagiwara, Fukuda & Eaton, 1974) and snail neurones (e.g. Akaike *et al.* 1978). As in these other preparations, Ca^{2+} transport through our Ca^{2+} channel shows saturation, and it is blocked by Mg^{2+} at high concentrations. Our results differ from the above quoted ones in that Mn^{2+} is clearly permeant, as it is in ventricular cardiac muscle (Ochi, 1976). Also, small Mg^{2+} currents were seen by us. It seems reasonable to attribute them to the Ca^{2+} channel. However, we cannot rule out the possibility that the Mg^{2+} inward currents flow instead through a relatively unselective permeability mechanism which operates most strikingly in absence of divalent cations (Palade & Almers, 1978) and is blocked by Ca^{2+}, Sr^{2+} and Ba^{2+} but not very effectively by Mg^{2+} (results to be published elsewhere).

Voltage dependence and kinetics.

Study of these properties is hindered by the location of Ca^{2+} channels in the transverse tubular system (Almers *et al.* 1981) where the transmembrane potential is not readily measured or controlled. Therefore, we do not attempt a detailed kinetic analysis at this stage. It seems safe to say, however, that in fibres and under

conditions where kinetic parameters appeared not to depend critically on Ca^{2+} conductance, Ca^{2+} channels open extremely slowly under depolarization, but close rapidly under repolarization. At 15 mV, time-to-peak in our measurements is 100–300 msec, 30–100 times longer than in axotomized snail neurones (Akaike *et al.* 1978). Decline of I_{Ca} under repolarization is also slower than in snail neurones, though the difference is less (time constant about 10 msec here as opposed to 1–2 msec in snail neurones). I_{Ca} of vertebrate cardiac muscle has been studied in detail, most recently by McDonald & Trautwein (1978). In their work on cat cardiac trabeculae, I_{Ca} rose to a peak in 10 msec at 10 mV and 37 °C; assuming a reasonable Q_{10} of 3 for this process, one might expect a time to peak of 50 msec at the temperature of our experiments (20–22 °C), at least twice faster than observed here. On the other hand the decline of I_{Ca} under repolarization of cat ventricles occurred with a time constant of about 200 msec at 24 °C, twenty times more slowly than in our work. Compared to Ca^{2+} channels in cardiac muscle, those investigated here open more slowly and, upon repolarization, close much more rapidly. The kinetic properties found here may have their physiologic significance in limiting Ca^{2+} entry during an action potential. While in the heart Ca^{2+} entry plays an important role for action potential and excitation–contraction coupling, it has no clear significance of this kind in skeletal muscle. Skeletal muscle is well known to rely predominantly or entirely on internal stores for regulating cytoplasmic Ca^{2+} concentration, at least during twitches and short tetani.

Extra Ca^{2+} influx elicited by an action potential

Extra influx was measured in Ringer fluid with $^{45}Ca^{2+}$ by Bianchi & Shanes (1959; 0·2 p-mole/cm^2 . twitch, whole frog sartorius) and Curtis (1966; 1 p-mole/cm^2 . twitch, single fibres of frog semitendinosus). The greater part of any extra influx through the Ca^{2+} channel would be expected to occur as an inward 'tail' of I_{Ca} following the action potential, perhaps coinciding roughly with the early after-depolarization (see, e.g. Adrian & Peachey, 1973). After a strong depolarization expected to open all channels, the 'tail' current in Fig. 11*A* carried a charge of about 0·5 C/l. of fibre volume, equivalent to a Ca^{2+} entry of 2·6 μmole/l. If an action potential in the transverse tubules is equivalent to a 2 msec depolarization to 25–30 mV, it might open about $100 \times (1\text{-}\exp(-2/55))\% = 4\%$ of all Ca^{2+} channels in a fibre where channels open exponentially, with a time constant of 55 msec at that potential, as in Fig. 11. Repolarization would then elicit a tail current carrying 0·1 μmole/l. of Ca^{2+} in our 10 mM-Ca^{2+} solution. In Ringer fluid, the Ca^{2+} activity is six times less, so that one may expect a Ca^{2+} influx of perhaps 15 n-mole/l. fibre volume. In the same units, the influxes measured with $^{45}Ca^{2+}$ amount to between 540 n-mole/l. (Curtis, 1966; average fibre diameter 74 μm) and 108 n-mole/l. of fibre volume (Bianchi & Shanes, 1959; assuming 74 μm fibre diameter), an order of magnitude higher than expected from the channel we have studied. Some of the total measured tracer flux may occur through pathways other than the Ca^{2+} channel described here. The point cannot be pressed, however, due to the many differences between experimental conditions in ours and the isotope experiments.

Slow outward currents

Studying inward K^+ current tails in intact fibres, Adrian, Chandler & Hodgkin (1970*b*) have inferred the existence of a slow K^+ conductance system which is postulated to produce a K^+ current that rises to a peak of 0·2 mA/cm^2 within 1–2 sec during depolarization to −13 mV and slowly declines thereafter (their Fig. 3). This kinetic behaviour would be similar to that of our K^+ outward current seen, e.g. in Figs. 1–3. Stanfield (1970) observed a similar slow current and found that it is resistant to block by external TEA^+, as is ours. However, there is a possible difference between our K^+ currents and those thought to occur in intact fibres. Sanchez & Stefani (1978) find in intact fibres that all evidence of such a current vanishes when they replace external Ca^{2+} with Mg^{2+}. We find that such a replacement instead increases the outward current, as if the conductance mechanism in question were partly blocked by Ca^{2+} but not by Mg^{2+}. Outward currents of similar size were seen by us also when Ba^{2+} or Sr^{2+} replaced Ca^{2+}. More experiments are needed to explore this interesting difference between Sanchez & Stefani's (1978) result and our own. It may be related to the presence of internal EGTA in our experiments.

Fig. 2 appears to rule out the possibility that the late outward currents observed by us flow through a K^+ channel that is activated by internal Ca^{2+} (Meech, 1978). However, it does not rule out the existence of such a channel first suggested by Fink & Lüttgau's (1976) work on metabolically exhausted fibres. It seems possible that Ca^{2+}-activated K^+ currents were not seen by us simply because the high internal EGTA concentration in our fibres prevented internal Ca^{2+} from rising sufficiently.

We thank Drs D. Adams and B. Hille for their comments on the manuscript and Dr R. Fink for help with micro-electrode measurements. P.T.P. held a research fellowship from the Muscular Dystrophy Association of America, Inc. The work was supported by USPHS grant no. AM-17803.

REFERENCES

ADAMS, D. J. & GAGE, P. W. (1979). Sodium and calcium gating currents in an *Aplysia* neurone. *J. Physiol.* **291**, 467–481.

ADRIAN, R. H. & ALMERS, W. (1976). Charge movement in the membrane of striated muscle. *J. Physiol.* **254**, 339–360.

ADRIAN, R. H., CHANDLER, W. K. & HODGKIN, A. L. (1970*a*). Voltage clamp experiments in striated muscle fibres. *J. Physiol.* **208**, 607–644.

ADRIAN, R. H., CHANDLER, W. K. & HODGKIN, A. L. (1970*b*). Slow changes in potassium permeability in skeletal muscle. *J. Physiol.* **208**, 645–668.

ADRIAN, R. H. & PEACHEY, L. D. (1973). Reconstruction of the action potential of frog sartorius muscle. *J. Physiol.* **235**, 103–131.

AKAIKE, N., FISHMAN, H. M., LEE, K. S., MOORE, L. E. & BROWN, A. M. (1978). The units of calcium conduction in *Helix* neurones. *Nature, Lond.* **274**, 379–382.

ALMERS, W., FINK, R. & PALADE, P. T. (1981). Calcium depletion in muscle tubules: the decline of calcium current under maintained depolarization. *J. Physiol.* **312**, 177–207.

ARMSTRONG, C. M. & BEZANILLA, F. (1975). Currents associated with the ionic gating structures in nerve membrane. *Ann. N.Y. Acad. Sci.* **264**, 265–277.

BEATY, G. N. & STEFANI, E. (1976). Calcium-dependent electrical activity in twitch muscle fibres of the frog. *Proc. R. Soc.* B **194**, 141–150.

BIANCHI, C. P. & SHANES, A. M. (1959). Calcium influx in skeletal muscle at rest, during activity, and during potassium contracture. *J. gen. Physiol.* **42**, 803–819.

CHANDLER, W. K., RAKOWSKI, R. F. & SCHNEIDER, M. F. (1976). A non-linear voltage dependent charge movement in frog skeletal muscle. *J. Physiol.* **254**, 245–283.

CURTIS, B. A. (1966). Ca fluxes in single twitch muscle fibres. *J. gen. Physiol.* **50**, 255–267.

FINK, R. & LÜTTGAU, H. C. (1976). An evaluation of membrane constants and the potassium conductance in metabolically exhausted muscle fibres. *J. Physiol.* **263**, 215–238.

FRANKENHAEUSER, B. & HODGKIN, A. L. (1957). The action of calcium on the electrical properties of squid axons. *J. Physiol.* **137**, 218–244.

HAGIWARA, S. (1975). Ca-dependent action potential. In *Membranes*, vol. 3. ed. EISENMAN, G., New York: Dekker Inc.

HAGIWARA, S., FUKUDA, J. & EATON, D. C. (1974). Membrane currents carried by Ca, Sr and Ba in barnacle muscle fiber during voltage clamp. *J. gen. Physiol.* **63**, 564–578.

HILLE, B. & CAMPBELL, D. T. (1976). An improved vaseline gap voltage clamp for skeletal muscle fibers. *J. gen. Physiol.* **67**, 265–293.

HILLE, B., WOODHULL, A. M. & SHAPIRO, B. I. (1975). Negative surface charge near sodium channels of nerve: divalent ions, monovalent ions, and pH. *Phil. Trans. Roy. Soc.* B **270**, 301–318.

HODGKIN, A. L. & HOROWICZ, P. (1959). The influence of potassium and chloride ions on the membrane potential of single muscle fibres. *J. Physiol.* **148**, 127–160.

HODGKIN, A. L. & NAKAJIMA, S. (1972*a*). The effects of diameter on the electrical constants of frog skeletal muscle fibres. *J. Physiol.* **221**, 105–120.

HODGKIN, A. L. & NAKAJIMA, S. (1972*b*). Analysis of the membrane capacity in frog muscle. *J. Physiol.* **221**, 121–136.

KOSTYUK, P. G. & KRISHTAL, O. A. (1977). Separation of sodium and calcium currents in the somatic membrane of mollusc neurones. *J. Physiol.* **270**, 545–568.

KOSTYUK, P. G., KRISHTAL, O. A. & PIDOPLICHKO, V. I. (1978). Estimation of conductance of a single calcium channel from current fluctuations with the aid of the EGTA effect. *Dokl. Akad. Nauk SSSR* **238**, 478–481.

KRISHTAL, O. A. & PIDOPLICHKO, V. I. (1976). Displacement currents connected with the activation of gating mechanism of calcium channels in nerve cell membrane. *Dokl. Akad. Nauk SSSR* **231**, 1248–1251.

MCDONALD, T. F. & TRAUTWEIN, W. (1978). Membrane currents in cat myocardium: Separation of inward and outward components. *J. Physiol.* **274**, 193–216.

MEECH, R. W. (1978). Calcium-dependent potassium activation in nervous tissues. *Annu. Rev. Biophys. Bioeng.* **7**, 1–18.

OCHI, R. (1976). Manganese-dependent propagated action potentials and their depression by electrical stimulation in guinea-pig myocardium perfused by sodium-free media. *J. Physiol.* **263**, 139–156.

PALADE, P. T. & ALMERS, W. (1978). Slow Na^+ and Ca^{2+} currents across the membrane of frog skeletal muscle fibres. *Biophys. J.* **21**, 168a.

REUTER, H. (1973). Divalent cations as charge carriers in excitable membranes. *Prog. Biophys, molec. Biol.* **26**, 1–44.

SANCHEZ, J. A. & STEFANI, E. (1978). Inward calcium current in twitch muscle fibres of the frog. *J. Physiol.* **283**, 197–209.

STANFIELD, P. R. (1970). The effect of the tetraethylammonium ion on the delayed currents of frog skeletal muscle. *J. Physiol.* **209**, 209–229.

STANFIELD, P. R. (1977). A calcium-dependent inward current in frog skeletal muscle fibres. *Pflügers Arch.* **368**, 267–270.